

Enhanced Deep CNN Based Arithmetic Optimization Algorithm for Acute Myelogenous Leukemia Detection

1V.Jeya Ramya, 2Dr.S.Lakshmi

1Research scholar, Sathyabama Institute of Science and Technology, Chennai, India.

2 Associate Professor, Sathyabama Institute of Science and Technology, Chennai, India.

Abstract

Leukemia is the kind of cancer caused in bone marrow due to the immature leukocytes. The manual blood testing method is a slow process and required more time with less accurate detection results. Several methods are available for the detecting AML from the images of blood cell. The major motive of this work is for developing the efficient technique for leukemia detection. The proposed approach developed the enhanced Deep CNN with arithmetic optimization algorithm based leukemia detection from the peripheral blood cell images. Here, AML is detected by the process namely pre-processing phase, segmentation phase, feature extraction phase, and classification phase. In the pre-processing phase, the unwanted noises and redundant data are removed. The nucleus as well as masked cell image is segmented by utilizing the modified distance regularized level set evolution (DRLSE) algorithm. Then the feature extraction as well as the classification is carried out by the DCNN for the recognition of the normal images and also the AML infected images. The classification accuracy and the performance are improved by the arithmetic optimization algorithm. The analysis is carried out by utilizing the image from Munich AML Morphology Database and CPTAC-AML and performance is computed depends upon the metrics such as accuracy, precision, sensitivity, and specificity. The experimental results revealed that the proposed DCNN-AOA classifier has achieved the highest accuracy of 99.82%. The performances of the proposed classifier are compared to other approaches and the analysis shows that this method provides better performance when compared to other methods.

Keywords: Leukemia, acute myeloid leukemia (AML), bone marrow, segmentation, modified DRLSE, classification, Deep CNN, Arithmetic optimization algorithm,

1. INTRODUCTION

A white blood cell performs the significant part in the detection of various diseases hence the information extractions regarding diagnosis purpose is helpful for clinicians. It represents blood cancer, and the detection of leukemia depends upon the point that the count of the white cells is maximized by the blast cells that are immature and reduced neutrophil [1]. The stem cells are extremely tiny but able to duplicate the white blood cell numbers, platelets, and red blood cells whenever motivated. The stem cells consist of two groups, the first group represents myeloid stem cells which emerge into leukocytes, platelets, and erythrocytes and the next group is the lymphoid stem cells that is emerged into other type of leukocytes called B-cells as well as T-cells [2].

Leukemia is the form of cancer that damages the WBCs. Leukemia affected patients contain huge amount of irregular WBC. The unnecessary WBC quantity results in the reduction of healthy blood cells. It is the group of several blood disorders originated in the bone marrow so

their regular WBC are not in the matured type called blast cells [3]. Acute leukemia is a type of the cancer that expands quickly and makes bad suddenly whereas, chronic leukemia expands gradually and makes worst slowly concerning the time. Leukemia is identified by calculating the total blood cell numbers and then the RBC numbers and WBC numbers are compared by haematologists. Hence, the process of computing the blood cells with the help of a microscope is tiring and time-consuming [4]. The image detection using a microscope contains various outcomes and cannot have apparent standards because the process depends on the haematologist's knowledge. The other methods utilized for computing the blood cell counts are flow cytometer, molecular probing, and immunophenotyping are utilized as the standard leukemia investigation but this method is regarded as costly [5]. AML is considered as the common leukemia in grown person by 3 to 5 cases per 100,000 peoples. About 20,000 new cases are detected in a year, half of them have died from this disease. AML is the hematopoietic malignancy which has high number of cases and also has high mortality. It is common in adults aged more than 65 years and about 16-21% of childhood leukemia. The primary detection and treatment are important for the reduction of the death rate of the patients [6].

The world health organization published the revisions of acute leukemia and myeloid neoplasms in 2016. The updated classification in 2016 integrates the medical attributes, cytogenetics, molecular genetics, and immunophenotyping to describe the disease creatures with clinical importance [7]. The fundamental protocol demonstrates the process for tagging the bone marrow or peripheral blood cells. This tagging is done by the integration of antibodies which permits instantaneous dissection of standard hematopoietic maturation and detection of residual AML. It is composed of the support protocol arguing the methods utilized for the understanding of the resultant flow cytometric data. The traditional detection method is the elaborated examination of blood components and the bone marrow biopsy. The latter one is painful and the persistent process that provides the psychological disturbance and other linked discomforts [8].

The bone marrow biopsy results are not provided earlier in some of the general hospitals. This causes emotional stress, a bit like hanging loose in the hot air. The patients have the risk of death before the treatment, when the diagnosis results are late [9]. The blood cell image recognition as well as the identification by the automated system includes the cell segmentation, morphological feature extraction, and classification. The segmentation of cells is a major role in the detection of AML. The segmentation of cell is to detect the nucleus and cytoplasm edges. The ratio of the nucleus or cytoplasm is more significant for the blast recognition and the detection of AML [10]. This paper proposes the novel method for the detection of AML from the image groups by four processes, pre-processing, segmentation phase is using modified distance regularized level set evolution (DRLSE) algorithm, feature extraction the classification process using Deep CNN with the arithmetic optimization algorithm. The major contributions of the paper are

- Segmenting the nucleus by using modified distance regularized level set evolution approach
- Proposing the DCNN for the accurate acute myeloid leukemia images classification.
- Utilizing the arithmetic optimization algorithm for the enhancement of the classification accuracy and also to enhance the performance of the classifier.

The remaining sections of the paper are as pursues. Section 2 depicts the existing work summary regarding AML detection. The proposed methodology for the detection of AML is explained in

Section 3. Section 4 articulates the dataset, performance measures, and performance analysis. Section 5 finishes the paper.

2. SUMMARY OF EXISTING WORKS

Through the last two decades, associates are working dynamically in the medical image processing area and proposed several methods. The main steps in the automated detection are white blood cell segmentation for the extraction of the cytoplasm and nucleus pursued by feature extraction as well as classification. This section describes the literary works about acute myelogenous detection and described in Table 1. Su J et al. (2017) proposed a Hidden Markov Random Field (HMRF) for the detection of AML from the 61 bone marrow aspirate images. The performance measures such as accuracy and efficiency were evaluated using this method. The identification of blast for the AML detection was not possible using this method [11].

Aypar et al. (2019) proposed next-generation sequencing (NGS) to detect the structural abnormalities and copy number alterations for enhancing the diagnostic yield for the patients suffered from AML. The data collected from 20 karyotypically -normal AML and 68 known -abnormal samples for the performance evaluation purpose. Accuracy is the performance measure for the recognition of AML. The new abnormalities during the genome linked with myeloid malignancies detection were difficult [12].

Harjoko A et al. (2018) proposed Momentum Backpropagation artificial neural network and Active Contour with no Edge (ACWE) for the classification of subtypes of AML. The database of 734 data obtained from Dr. Sardjito Hospital Yogyakarta. Accuracy, precision, sensitivity, and specificity were the measures utilized for the performance evaluation [13].

Matek C et al. (2019) proposed a Convolutional neural network for the leukocyte classification and the performances of the network is evaluated when compared with inter and intra-expert inconsistency. The database of 100 patient's detected with various AML subtypes at the Leukemia Diagnostics Laboratory at Munich University Hospital among 2014 and 2017. The performance measures such as precision, sensitivity, and specificity were utilized for the evaluation purposes. This method has poor performance and difficult to diagnose the haematological malignancies [14].

Rawat J et al. (2017) proposed an SVM classifier by the kernel function for the analysis of myeloid and lymphoid cells. 420 blood microscopic images obtained from the online hematology in American society was the database employed for the performance evaluation. The performance measures such as accuracy and Cohens Kappa value utilized for the evaluation purposes. The major drawback of this method was low quality and low precision [15].

Kaur J et al. (2018) implemented the K-means clustering method for the classification of cells and the Independent component analysis (ICA) algorithm is utilized for the extraction of features. The feed-forward neural network was employed for the classification of cancer detection. The database was collected from the ALL-DB site and UCI machine repository. The performance measures such as false acceptance rate, accuracy, false rejection rate, and mean square error were computed for the performance evaluation. This method was not possible to describe the accurately described highlighted extraction process [16].

Agaian et al. (2014) proposed SVM and cross-validation mechanically identifies and segments the AML in blood smear images. The database of 80 images acquired from the American Society of Hematology (ASH). The measures namely sensitivity, precision, F-measure and specificity were

utilized for the performance evaluation purposes. Gathering more samples to obtain better performance was difficult using this method [17].

Kumar P et al. (2017) projected the new technique was examined to identify the presence of AML. The microscopic blood smear images were obtained from the American Society of Haematology (ASH) were utilized as database. Execution time and accuracy were the measures utilized for the performance evaluation. The SVM was the classifier utilized for the classification of AML detection. Different subtypes of AML were not possible to detect using this method [18].

Table 1: Literary works about the AML detection

References	Method	Database	Measures	Limitations
Su J et al. (2017) [11]	Hidden Markov Random Field (HMRF)	61 bone marrow aspirate images	Accuracy and efficiency	Difficult to identify the blast for the AML detection
Aypar U et al. (2019) [12]	NGS based methodology	20 karyotypically - normal and 68 known - abnormal AML samples	Accuracy	Difficult to detect new abnormalities during the genome linked with myeloid malignancies
Harjoko A et al. (2018) [13]	Active Contour Without Edge (ACWE) approach and Momentum Backpropagation artificial neural network technique	734 data attained from Dr. Sardjito Hospital Yogyakarta via ethical clearances	Accuracy, precision, sensitivity and specificity	Less sensitive to input image
Matek C et al. (2019) [14]	Convolutional neural network	100 patients detected with various AML subtypes at the Leukemia Diagnostics Laboratory at Munich University Hospital in between 2014 and 2017	Precision, sensitivity and specificity	Poor performance and difficulty to diagnose the hematological malignancies
Rawat J et al. (2017) [15]	SVM classifier with kernel functions	420 blood images obtained from the online repository offered by the hematology in American society	Accuracy, Cohens Kappa value	Low quality and precision.

Kaur J et al. (2018) [16]	ICA feature extraction Feed-Forward neural network	ALL-DB site and UCI MACHINE REPOSITORY	accuracy, Mean square error	Accurately describing highlight extraction process was not possible
Agaian S et al. (2014) [17]	SVM and cross-validation	80 images obtained from American Society of Hematology (ASH)	Precision, sensitivity, specificity and F-measure	Gathering more samples to obtain better performance was difficult
Kumar P et al. (2017) [18]	SVM	Blood smear images obtained from the American Society of Hematology (ASH)	Execution time, accuracy	Different subtypes of AML was not possible to detect

3. PROPOSED METHODOLOGY

In this proposed approach, the four phases are elucidated; pre-processing phase, segmentation phase, feature extraction phase, and classification phase. Initially, in the pre-processing stage, the unwanted noise signals are removed and the image quality is improved. The second phase is the segmentation process in which the nucleus is segmented from the whole dataset. For the process of segmentation, the modified regularized level set evolution approach is utilized. The next phase is the feature extraction as well as the classification process. In the classification process, the AML cells and the normal cells are recognized by the deep convolutional neural network. The classification accuracy is enhanced by using the Arithmetic optimization algorithm. The block diagram of the proposed approach is portrayed in Fig 1. The detailed description of the proposed diabetic retinopathy detection is explained below.

Pre-processing

The images obtained from the digital microscope are typically in the color space of RGB in which the segmentation is complicated. The image environment and the blood cells significantly change with respect to the intensity and color. This occurred because of various causes like settings of the aging stain, camera and altering illumination [18]. To make the segmentation more robust regarding these changes, an adaptive scheme is utilized. The RGB is transformed to CIELAB. Next, only two color elements such as a^* and b^* are intended to estimate the human vision. At last, the color elements such as a^* and b^* are utilized to create the correct color balance improvements. In $D^*a^*b^*$ color space, the dimension D^* indicates the color lightness, dimension a^* indicates the location among the red and green, and the dimension b^* indicates the location blue and yellow. Because of its perceptual uniformity, $D^*a^*b^*$ creates the visual alterations in the identical amount of the color value. The pre-processing stage is utilized to eradicate the annoying noise from the obtained image. The entire input image color information is indicated in a^* and b^* . Thus, the image from the pre-processing stage is utilized for the segmentation of nucleus.

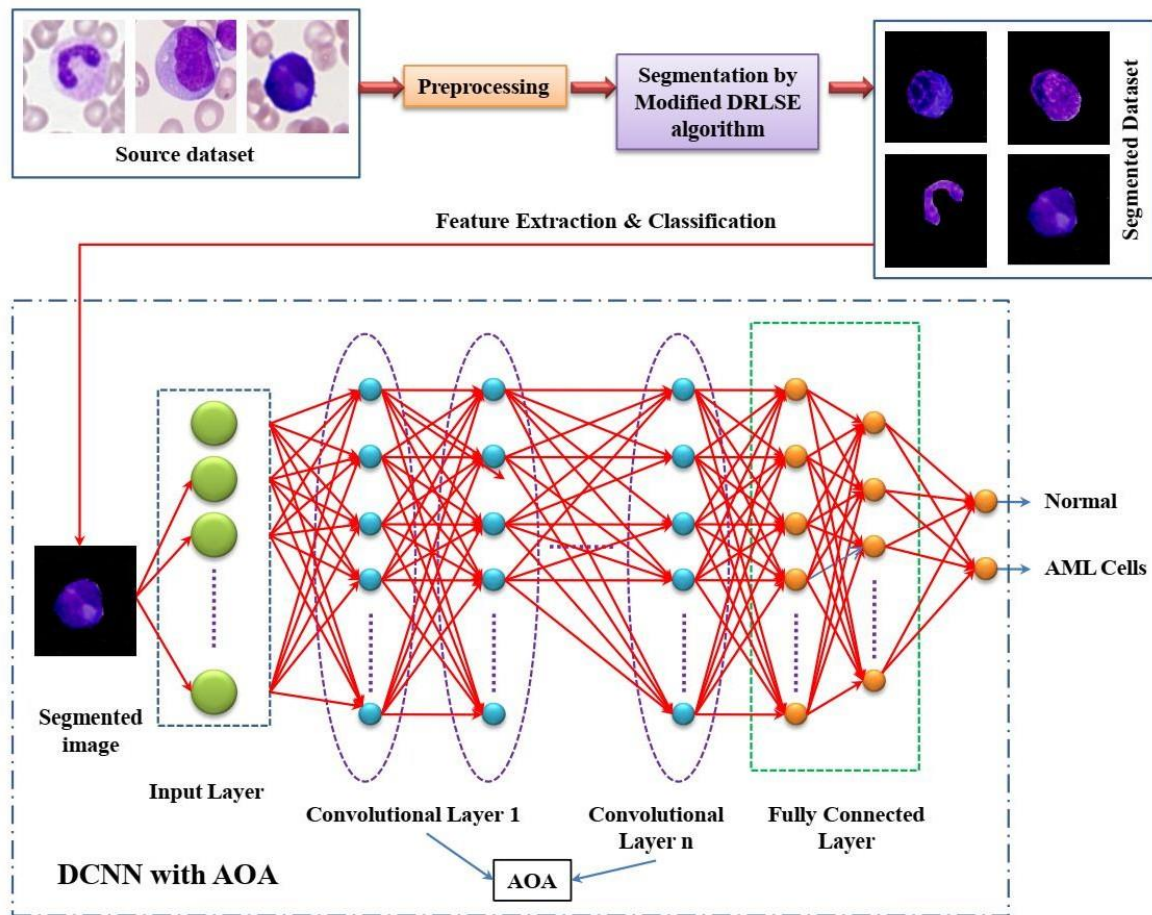


Fig 1: Block diagram of proposed AML detection

Segmentation

The main objective of image segmentation is for extracting the significant data from the input. The segmentation method plays an important position because the proficiency of the consequent feature extraction as well as the classification depends upon the myeloblasts precise recognition. For the accurate nucleus segmentation, the modified DRLSE[36] technique is utilised.

3.2.1. Modified DRLSE:

The distance regularized has several merits when compared with the traditional level set method, with respect to initialization. It directs to the imperfect nucleus segmentation when it contains both weak and sharp edges appeared at various areas of the nucleus. When weak boundary is occurred in conjunction with little alterations in the concentrations, it is not perfectly identified by the edge indicator that leads to inaccurate segmentation. Hence, this research proposed the integration of the Region scalable fitting (RSF) concept in the DRLSE [20] for the improved segmentation. RSF-based segmentation operates in weak edges because it accounts for regional intensity information however suffers from the process of re-initialization [23]. RSF [22] applied on the DRLSE that enhances the time and the computational complexity [24].

The level set formulation [21] (LSF) has the edge and region-based fitting energy factor, then the regularisation factor is for evading the difficult re-initialisation scheme. It decreases the computational complexity because it contains only intensity data integrated to the DRLSE equation in place of

simply merging into the structure. This segmentation method is to conquer the drawbacks of the DRLSE method.

The functional equation of the energy is achieved by integrating the RSF and DRLSE. The region scalable fitting (RSF) factor is expressed as:

$$\alpha(\phi) = \beta_1 \int_{\Omega} L_{\sigma}(a-b) |J(b) - F_1(a)|^2 * N_1[\phi(b)] db + \beta_2 \int_{\Omega} L_{\sigma}(a-b) |J(b) - F_2(a)|^2 * N_2[\phi(b)] db \quad (1)$$

From Eqn. (1), $\alpha(\phi)$ represents the energy functional, α represents the constant, β_1 and β_2 represents the positive constants, $J(b)$ represents the intensity of the image included in the above fitting energy, $F_1(a)$ and $F_2(a)$ represents the two values that estimated the intensity of the image in the fields Ω_1 and Ω_2 , L_{σ} represents the function of the non-negative kernel.

The equation of the DRLSE for LSF is represented as

$$\alpha_{\alpha}(\phi) = \eta \int_{\Omega} q |\nabla \phi| da + \beta \int_{\Omega} h \delta_{\alpha}(\phi) |\nabla \phi| da + \nu \int_{\Omega} h G_{\alpha}(-\phi) da \quad (2)$$

From Eqn. (2), q represents the potential function, $\eta > 0$ represents the constant, $\beta > 0$ represents the coefficient of the area factor, ν represents the coefficient of the weighted area factor. The role of h in the energy factor is slowing down whenever the zero-level contour expands or shrinks. When it reaches the object edges the term h obtains the smaller values. The term δ and G represents the Dirac delta function as well as the Heaviside functions correspondingly.

The approximations for the line as well as the area factor in the DRLSE structure is represented as

$$\beta_1 \int_{\Omega} L_{\sigma}(a-b) |J(b) - F_1(a)|^2 * N_1[\phi(b)] db \approx \beta \int_{\Omega} h \delta_{\alpha}(\phi) |\nabla \phi| da \quad (3)$$

$$\beta_2 \int_{\Omega} L_{\sigma}(a-b) |J(b) - F_2(a)|^2 * N_2[\phi(b)] db \approx \beta \int_{\Omega} h G_{\alpha}(-\phi) da \quad (4)$$

The resultant equation is formed by integrating Eqns. (2), (3) and (4).

$$\alpha(\phi) = \mu S_q(\phi) + \beta \int_{\Omega} h |J(b) - F_1(a)|^2 * N_1[\phi(b)] db + \nu \int_{\Omega} h |J(b) - F_2(a)|^2 * N_2[\phi(b)] db \quad (5)$$

From Eqn. (5), N_1 and N_2 represents the Heaviside as well as the Dirac delta function described in the 2nd factor and the 3rd factors of Eqn. (2) that is employed in the resultant evaluation. In Eqn. (5), the edge indicator factor h is obtained from the DRLSE structure, $h |J(b) - F_1(a)|^2 * N_1[\phi(b)] db$ represents the estimation of the regional intensity obtained from the RSF structure from field 1 (within the boundary), and $h |J(b) - F_2(a)|^2 * N_2[\phi(b)] db$ represents the estimation of the regional intensity obtained from the structure of RSF from field 2 (outer boundary surface). The DRLSE boundary indicator scheme utilized here is $h = \text{boundary indicator}$.

$$L_{\sigma}(a-b) = h \quad (6)$$

AML detection using Improved Deep CNN

The discriminative features play a significant part in the classification process. There are several features that confuses the classifier and very few features are not adequate for the classification

perfectly. For the classification, train and test the various features and classifiers. The classifier is organized corresponding to the data intended for the effective outcomes, so the data is classified into the training database as well as the testing database. This paper proposes the deep learning method with CNN for the classification of AML cells and the normal cells. The final DCNN three layers are fully connected layer, SoftMax layer and the classification layer, and fine-tuned for the new layer of the classifier. These segmentation output is given to the proposed Deep CNN for the acute myeloid leukemia (AML) cells classification and the normal cells. This proposed classifier establishes the classification, and with the help of Arithmetic optimization algorithm (AOA), the accuracy of the classifier is enhanced. The architecture of the proposed DCNN with the AOA classifier is described in Fig 2.

Framework of the proposed DCNN classifier

The structure for the detection of AML classifier is described in Fig 2. The optimum weights are established using the optimization achieving proper classification results. The fundamental framework of the DCNN is concisely described [25]. The developed from of CNN is Deep CNN and hence the deep learning is promoted. Deep CNN consists of convolutional layers, fully connected layers and pooling layers. Once the features are extracted from the samples of the segmentation, then it is given to the convolutional layer. The convolutional layer intends to develop the classification of AML map. Next, the map of the feature tolerates the subsampling in the pooling layer and lastly, the fully connected layer executes the AML categorization. Every layer is supplied by the factors of weight based kernel for the output collection.

Convolutional layer: This layer obtains the attributes from the output of the segmentation. DCNN consists of the convolutional layer sequences. The feature vectors and the trained weights are integrated to establish the Convolutional layers feature map. This layer forwards the data to the next layer via the activation function. The value of the input vector coming to the Deep CNN convolutional layer is expressed as,

$$c = \{c_1, c_2, \dots, c_q, \dots, c_n\} \quad (7)$$

From Eqn. (7), n represents the total convolutional layer numbers is utilized in the DCNN, and c_q represents the DCNNs q^{th} convolutional layer. The convolutional layer output is expressed as,

$$(O_d^q)_{g,h} = (Y_e^q)_{g,h} + \sum_{p=1}^{K^{p-1}} \sum_{e=-m_1^k}^{m_1^k} \sum_{f=-m_2^k}^{m_2^k} (H_{d,p}^q)_{g,h} * (O_d^q)_{g+e,h+f} \quad (8)$$

Where $*$ represents the convolutional operator, $(O_d^q)_{g+e,h+f}$ represents the feature map given as the input, K^{p-1} indicates the features obtained from the earlier layer, $(Y_e^q)_{g,h}$ represents the convolutional layer bias, and $(H_{d,p}^q)_{g,h}$ represents the weight of the convolutional layers.

Pooling layer and Rectified linear unit (ReLU): ReLU layer contain the activation function used for adjusting the convolutional layer outputs. In addition to this, the rectified linear unit layer assures efficiency and hence it assists in trading the large networks. The ReLU output is expressed as,

$$O_d^q = F_n(O_d^{q-1}) \quad (9)$$

From Eqn. (9), $F_n(\cdot)$ represents the q^{th} layer activation function offered. Next, the reactivation linear unit output transmits in the direction of the pooling layer. The pooling layer practices the input via the local areas with no bias and weights.

Fully connected layers: For the classification of the image, the entire features are integrated in the last fully connected layer. Both the SoftMax layer and the classification layer is utilized for the classification. When the information is provided to the fully connected layer, the output is obtained from the pooling layer. The input is given to the fully connected layer for executing the classification as well as the output is expressed as,

$$C_e^q = T(y_e^q) \text{ with } y_e^k = \sum_{p=1}^{K^{p-1}} \sum_{g=1}^{K^{p-1}} \sum_{h=1}^{K^{p-1}} (P_{e,p,g,h}^q) \cdot (O_{g,h}^{q-1}) \quad (10)$$

From Eqn. (10), $P_{e,p,g,h}^q$ represents the weight linking (g,h) of the p^{th} feature map of the layer $q-1$ and e^{th} unit in the layer k . Every output of the three layers represents the weights that play an important role in the compilation of output. The deep CNN classifies the AML cells as well as the normal cells. For the optimal classification of the AML infected cells, utilize the Arithmetic optimization algorithm. This optimization algorithm is utilised to enhance of the DCNNs classification accuracy.

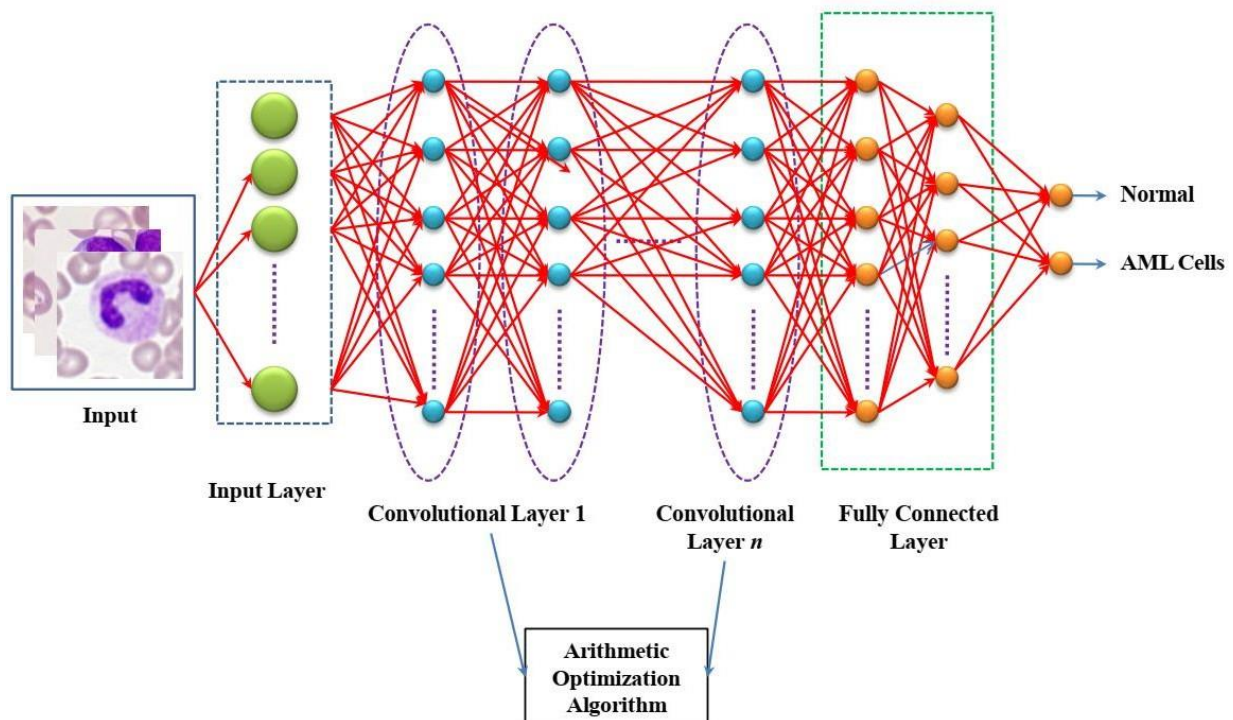


Fig 2: Structural Design of the proposed DCNN-AOA classifier

Arithmetic optimization algorithm

The arithmetic optimization algorithm is utilized with deep CNN to enhance the performance of the Deep CNN. This optimization algorithm is employed to improve the classification accuracy and also to improve the classification results. The global optimal solution is obtained by using an adequate number of arbitrary solutions as well as optimization repetitions. The optimization algorithm is composed of two main stages: exploration as well as exploitation. The exploration stage refers to the wide exposure of search space by the of the algorithm search agents to neglect the local solutions.

The exploitation stage provides the accuracy enhancement for the obtained solutions. The exploitation as well as the exploration stages are obtained by using arithmetic operators like addition (A), subtraction (S), multiplication (M), and division (D). This optimization algorithm is the population-based meta-heuristic algorithm that is used to solve the optimization issues devoid of computing their derivatives.

Inspiration:

Arithmetic is the main element of the number theory and it is the most significant part of the current mathematics, along with algebra, analysis, and geometry. The arithmetic operators are the conventional evaluation metrics utilized for studying the numbers [27]. The simple operators are utilized to compute the best component from the set of candidate alternatives. The behavior of the arithmetic operators and the manipulation of the proposed algorithm is discussed in the subsequent sub-sections.

Initialization:

The optimization procedure in the arithmetic optimization algorithm starts with the candidate solutions (U) sets depicted in the below matrix produced arbitrarily. The optimal candidate solution in every repetition is regarded as the optimal-achieved solution.

$$U = \begin{bmatrix} u_{1,1} & \cdot & \cdot & u_{1,k} & u_{1,1} & u_{1,m} \\ u_{2,1} & \cdot & \cdot & u_{1,k} & \cdot & u_{1,m} \\ \cdot & \cdot & \cdot & \cdot & \cdot & \cdot \\ \vdots & \vdots & \vdots & \vdots & \vdots & \vdots \\ u_{M-1,1} & \cdot & \cdot & u_{M-1,k} & \cdot & u_{M-1,m} \\ u_{M,1} & \cdot & \cdot & u_{M,k} & u_{M,m-1} & u_{M,m} \end{bmatrix} \quad (11)$$

The optimization algorithm chooses the search space before the algorithm begins to operate. Hence Math optimizer accelerated function (MOA) represents the coefficient computed using Eqn. (12) utilized in the subsequent search stages.

$$M_{OA}(P_Itr) = M_{in} + P_Itr \times \left(\frac{M_{ax} - M_{in}}{m_Itr} \right) \quad (12)$$

Where $M_{OA}(P_Itr)$ indicates the value of the function at the t th repetition that is computed as per the above equation. P_Itr represents the present iteration that lies among 1 and the highest iteration numbers m_Itr , M_{ax} and M_{in} represents the maximum and minimum accelerated function values correspondingly.

Exploration stage:

The exploratory behavior of the arithmetic optimization algorithm is explained in this section. The mathematical operators such as division or multiplication have the high distributed values that execute the exploration search method. These two operators cannot simply loom the goal because of their high dispersion when compared with other operators such as subtraction as well as the addition. The function is utilized that depends upon employing the four numerical operations to express the consequences of the various distribution value operator's. Thus the exploration stage search identifies the near-optimal solution which is assumed after various iterations. Moreover, the operators in the exploration stage such as division and multiplication are operated in the optimization stage to support exploitation stage in the process of search via the improved communication among them. The

operators in the exploration stage are to discover randomly search area on various areas and method to compute the optimal solution that depends upon the two major schemes like multiplication (M) search scheme as well as division (D) search scheme that are expressed in the below equation. The exploration searching stage is trained by the math optimizer accelerated function for the ailment $a1 < M_{OA}$ ($a1$ represents the arbitrary number). The first operator i.e., division operator (D) in this stage is trained by $a2 < 0.5$ and the other operator i.e., multiplication operator (M) is neglected till the first operator ends the present task. Else the second operator (M) is connected to execute the present task in place of D ($a2$ represents the arbitrary number). The subsequent equations are utilized for updating the position in the exploration stages of this paper.

$$u_{j,k}(P_Itr+1) = \begin{cases} best(u_k) \div (M_{OP} + \alpha) \times ((U_{b(j)} - L_{b(j)}) \times \beta + L_{b(j)}), & a2 < 0.5 \\ best(u_k) \times M_{OP} \times ((U_{b(j)} - L_{b(j)}) \times \beta + L_{b(j)}), & otherwise \end{cases} \quad (13)$$

From Eqn. (13), $u_{j,k}(P_Itr+1)$ represents the j th solution in the subsequent iteration, $u_{j,k}(P_Itr)$ represents the k th location of the j th solution at the present iteration, and $best(u_k)$ represents the k th location in the best-achieved solution, α represents the small integer number, $U_{b(j)}$ and $L_{b(j)}$ represents the value of the upper bound as well as the lower bound value of the k th location, correspondingly. β represents the control factor for adjusting the search scheme that is predetermined equal to 0.5 with respect to the experiment of this research.

Exploitation stage:

The exploitatory behavior of the arithmetic optimization algorithm is explained in this section. The mathematical operators such as addition (A) or subtraction (S) have the high dense values that consign to the exploitation search method. These two operators cannot simply reach the goal because of their low dispersion when compared with other operators such as subtraction as well as the addition. Thus the search in the exploitation stage identifies the near-optimal solution which is assumed after various iterations. Moreover, the operators in the exploitation stage such as addition and subtraction are operated in the optimization stage for supporting the exploitation stage via improved transmission among them. The exploitation search stage is prepared by the math optimizer value enhanced function for the ailment of $a1$ is not bigger than the present $M_{OA}(P_Itr)$ value. The operators of the exploitation like addition (A) or subtraction (S) of arithmetic optimization algorithms discover the search region genuinely on various opaque areas and the approach to evaluating the optimal solution depends upon the two major search schemes i.e., addition (A) search scheme or subtraction (S) search scheme that is described in Eqn. (14)

$$u_{j,k}(P_Itr+1) = \begin{cases} best(u_k) - M_{OP} \times ((U_{b(j)} - L_{b(j)}) \times \beta + L_{b(j)}), & a3 < 0.5 \\ best(u_k) + M_{OP} \times ((U_{b(j)} - L_{b(j)}) \times \beta + L_{b(j)}), & otherwise \end{cases} \quad (14)$$

The first operator (S) in the exploitation stage is adapted by $a3 < 0.5$ and the other operator (A) is ignored till this operator stops the present task. Elsewhere, the second operator (A) is connected to execute the present task in place of S . This process is the same as the partitions in the exploration stage. The exploitation search operators are strived to neglect getting jammed in the area of local search. This process helps the exploration search schemes in evaluating the best solution and observing the candidate solutions diversity. The parameter β is prudently intended to create the stochastic value at every repetition to sustain the exploration not only in the first iteration but also in

the final repetitions. This searching section is more useful in the local optima immobility circumstances, especially in the final repetitions.

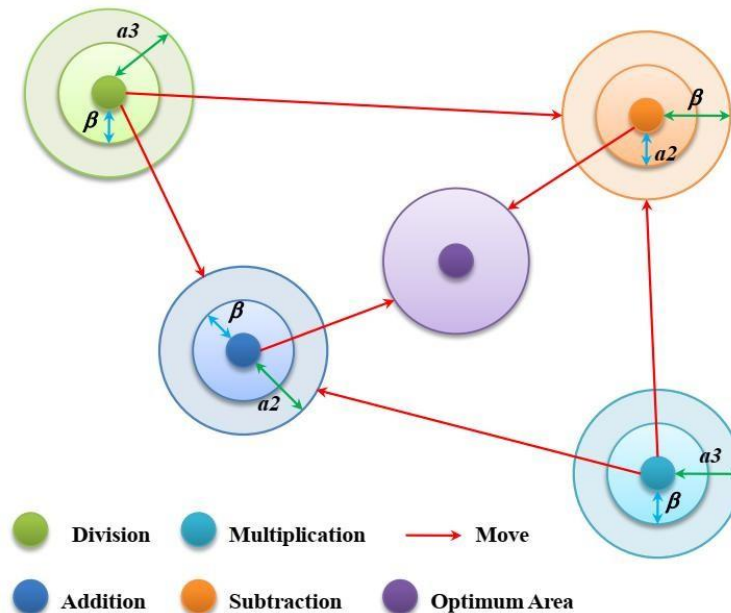


Fig 3: Structure for the location of arithmetical operators in AOA updated to the optimal region

Fig 3 portrays in what way the searching solution is updated the location with respect to M , D , A , and S in the 2-D search space. It is observed that the last achieved location is the stochastic location inside the interval that is described with the locations of M , D , A , and S in the search assortment. For the other models, M , D , A , and S computes the near-optimal solution location. The other solution is updated the locations approximately in the region near-optimal solution.

4. EXPERIMENTAL RESULTS AND DISCUSSIONS

This part describes the simulation results obtained from the proposed approach for AML detection available database namely Munich AML Morphology Dataset and CPTAC-AML. This section explains the proposed detection of AML using the classification of AML cells from the group of images implemented in the MATLAB platform with Windows 8 OS followed by 4GB RAM. The evaluation measures like accuracy, precision, F1-score, sensitivity, and specificity were utilized for the evaluation of the proposed classifier. The proposed approach performance is compared through the several existing methods for the detection of AML.

Dataset

The Munich AML morphology database consists of 18,365 solitary cell images obtained from the 100 patients peripheral blood cells detected with AML at Munich University Hospital [28] in the year from 2014 to 2017 and also CPTAV-AML datasets [29] are obtained from 88 patients with 120 images. The pathological as well as the non-pathological leukocytes are categorized into normal morphological classification methods described from the medical training by the qualified specialists. The sample database images are depicted in Fig 4.

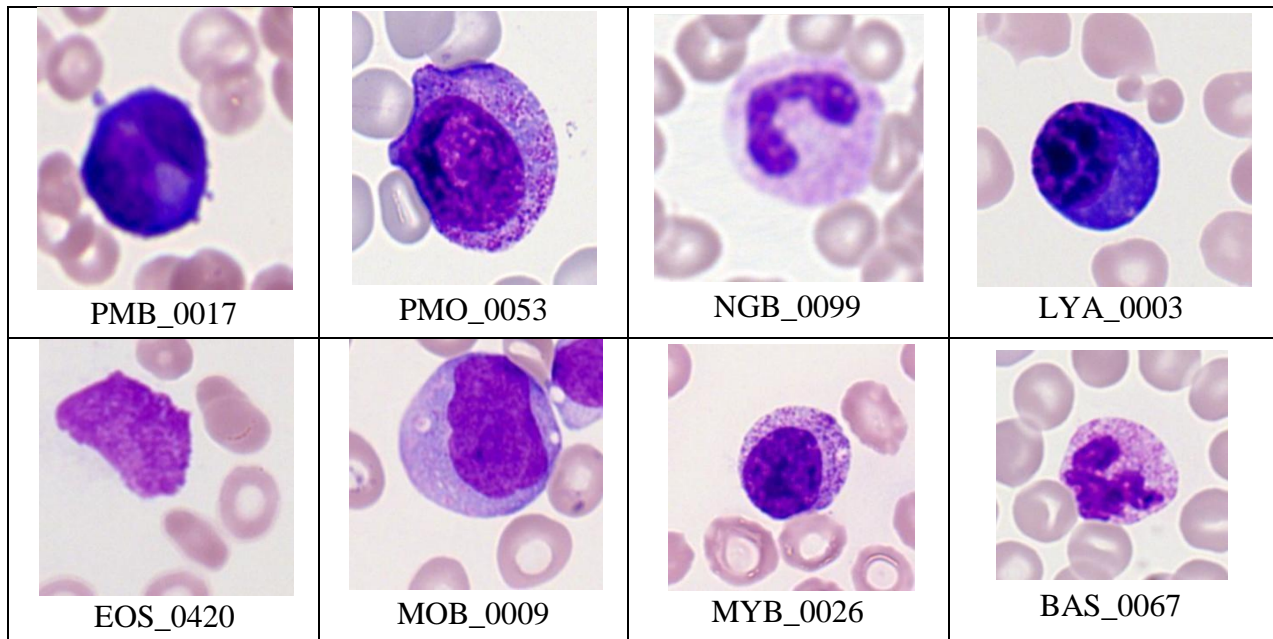


Fig 4: Sample images of the database

Performance measures utilized for the assessment

The performance measure depends upon the possible results of the classification: true negative, false positive, true positive, and false negative. The classification performance measures such as specificity, accuracy, precision, and sensitivity are described. The following measures are utilized for the assessment of the proposed approach.

Accuracy: It represents the exactly recognized diseases from the entire samples from the datasets. It describes how the approach appropriately or inappropriately reconstructs the high-resolution image.

$$Accuracy = \frac{tr_{po} + tr_{ne}}{tr_{po} + tr_{ne} + fa_{po} + fa_{ne}} \quad (15)$$

Where tr_{po} indicates the true positive, tr_{ne} indicates the true negative, fa_{po} indicates the false positive, fa_{ne} indicates the false negative.

Specificity: It is described as the true positive rate which is accurately detected by the classifier when testing. It is formulated as the below expression

$$Specificity = \frac{tr_{ne}}{tr_{ne} + fa_{po}} \quad (16)$$

Precision: It is the important metric for the determination of exactness, and it is described as positive that corresponds to the total predictive positive examples as expressed below

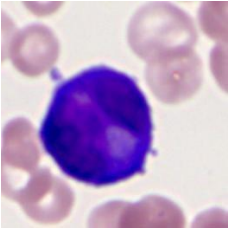


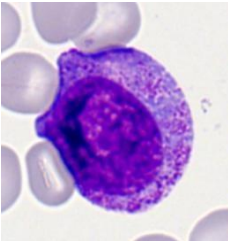


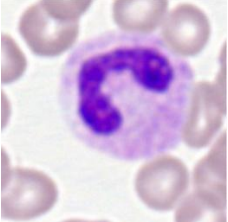

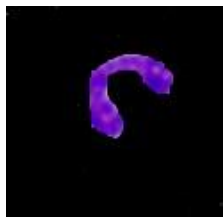
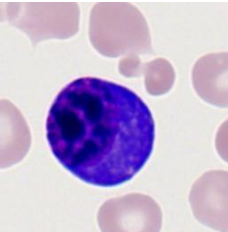


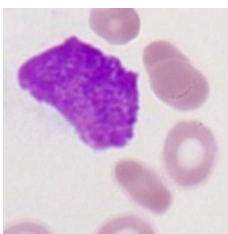


$$Precision = \frac{tr_{po}}{tr_{po} + fa_{po}} \quad (17)$$

Sensitivity: It is described as the true positive that is properly detected using the classifier during testing. It is expressed by the below equation.

$$Sensitivity = \frac{tr_{po}}{tr_{po} + fa_{ne}} \quad (18)$$

Segmentation results

The segmentation results for the proposed segmentation are depicted in Figure5. The modified DRLSE is the proposed segmentation method. By using this type of segmentation, accurate segmentation results are obtained. The segmented image is more efficient than any other segmentation methods.

Input Image	Masked image	Segmented nucleus
		
		
		
		
		

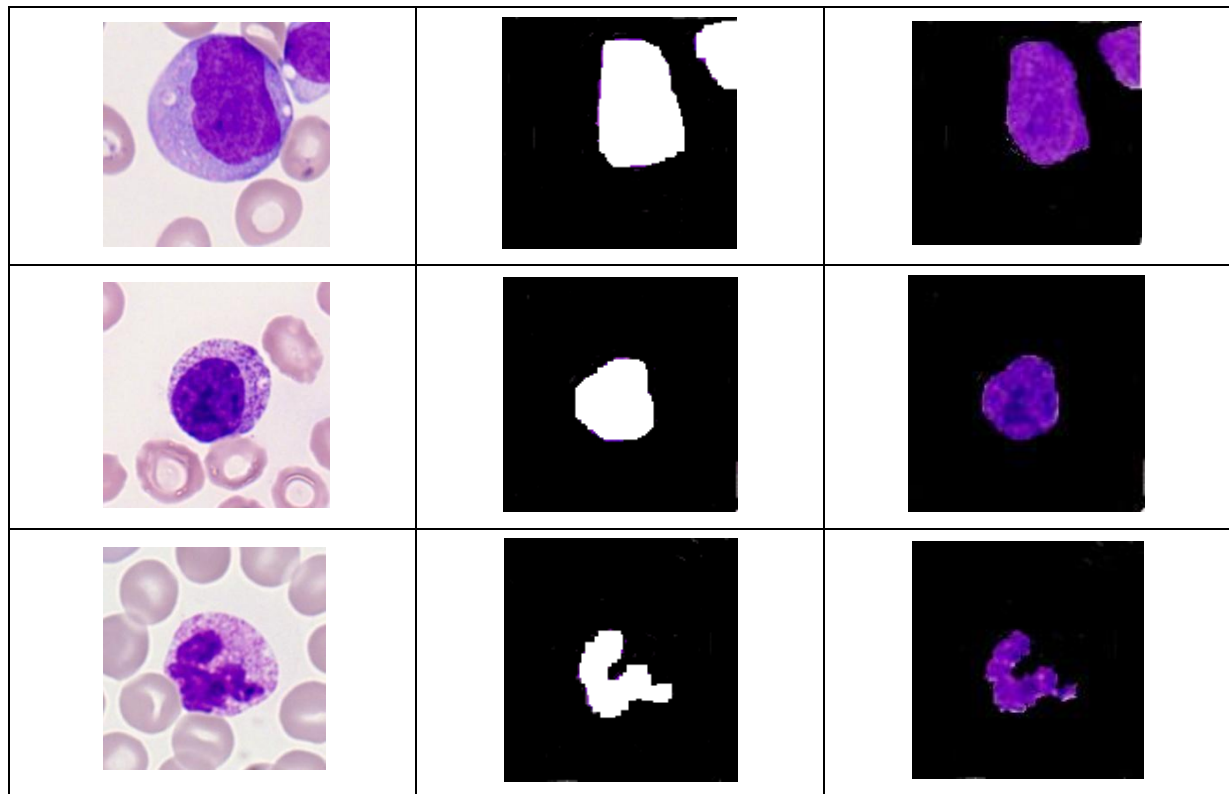


Fig 5: Segmentation of nuclei using Modified DRLSE method

Classification results

The classification results are computed on the testing database by the sensitivity, accuracy, and precision. In the process of classification, the true positive represents the image precisely provide the label, the true negative represents the mage is not perfectly provided the label, false-positive represents the image wrongly provide the label, and the false-negative represents the image wrongly provided the label. The Deep convolutional neural network with an arithmetic optimization algorithm is utilized for classification purposes. The optimization algorithm used in the DCNN is to enhance the classification accuracy and also to improve the algorithmperformance. The classification outcomes for the proposed approach with the other state-of-art method are compared and evaluated. The classification results for the detection of AML are evaluated with the measures like sensitivity, accuracy, specificity, and precision. Figure 6 reveals the training and validation results of the loss and accuracy. The loss and accuracy function for DCNN is exhibited by the graph for both the testing as well as the training dataset. The minimum loss and maximum accuracy values for both the testing as well as the training database are offered as well. In this, training was conducted for 100 times and the accuracy achieved is almost 100% in the process of training but the validation acquired is about 98%. In the loss progression, the process of training is established to be 0%, and validation achieves 12%.

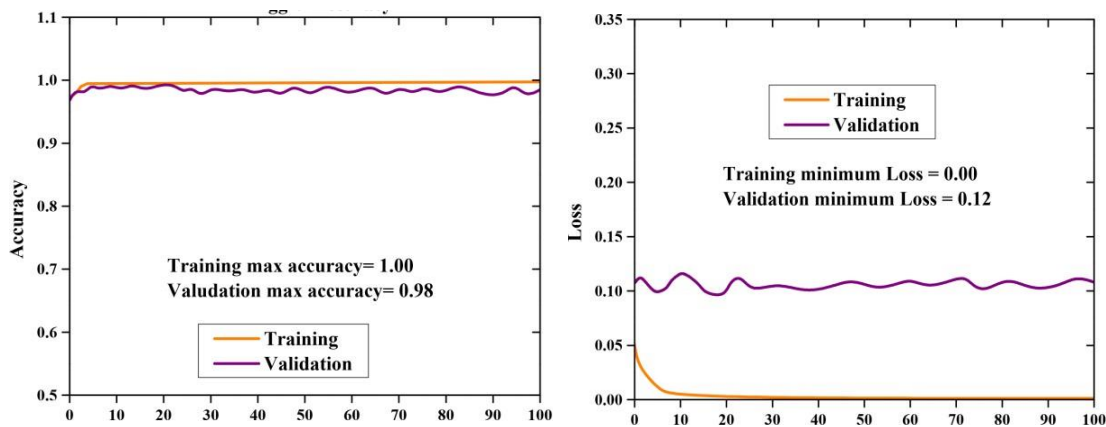


Fig 6: (a) Accuracy and (b) loss for the Deep CNN trained for 100 times

The comparative assessment of the proposed classifier with other existing classifiers namelyK-nearest neighbor (kNN) with Synthetic Minority Over-sampling Technique (SMOTE) [30], SVM [31], artificial neural network [32], and FBW-NN [33] is demonstrated in Table 2. Fig 7 describes the performance comparison of the different measures for the various classifiers. It is evident that the proposed classifier outperforms than any other classifiers.

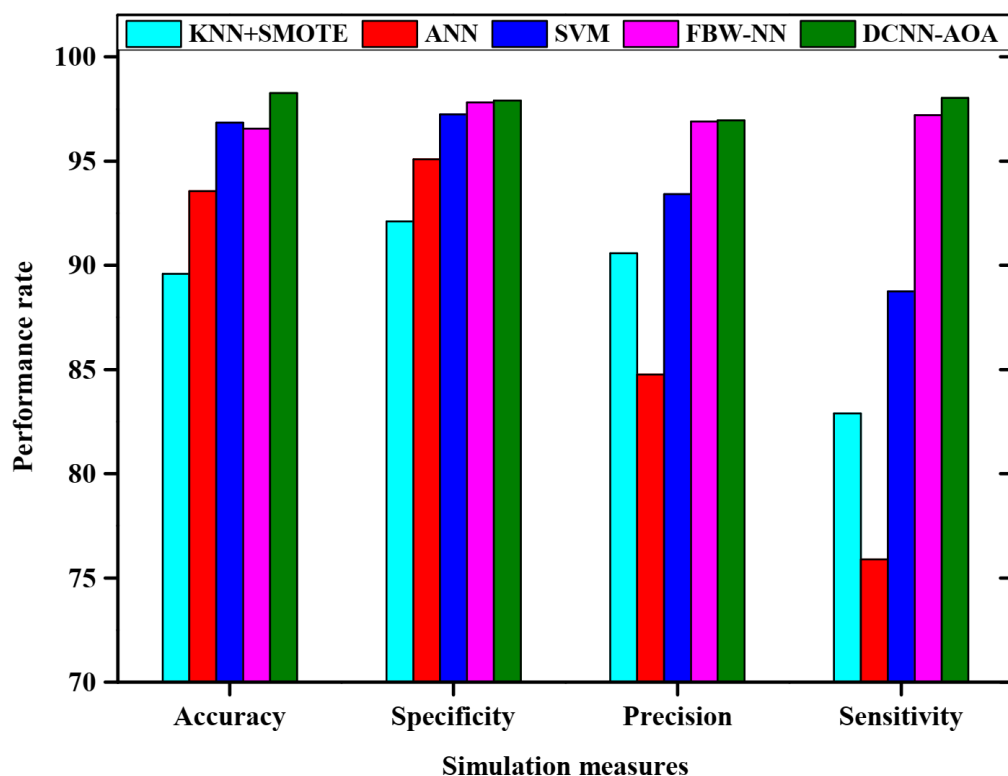


Fig 7: Comparative analysis of the measures for various classifiers

Table 3: Performance measures of the different classifiers

Classifiers	Accuracy	Specificity	Precision	Sensitivity
kNN + SMOTE	89.6%	92.1%	90.58%	82.9%
ANN	93.569%	95.090%	84.754%	75.887%
SVM	96.85%	97.24%	93.41%	88.75%

FBW-NN	96.56%	97.81%	96.90%	97.20%
DCNN-AOA	98.27%	97.91%	96.95%	98.04%

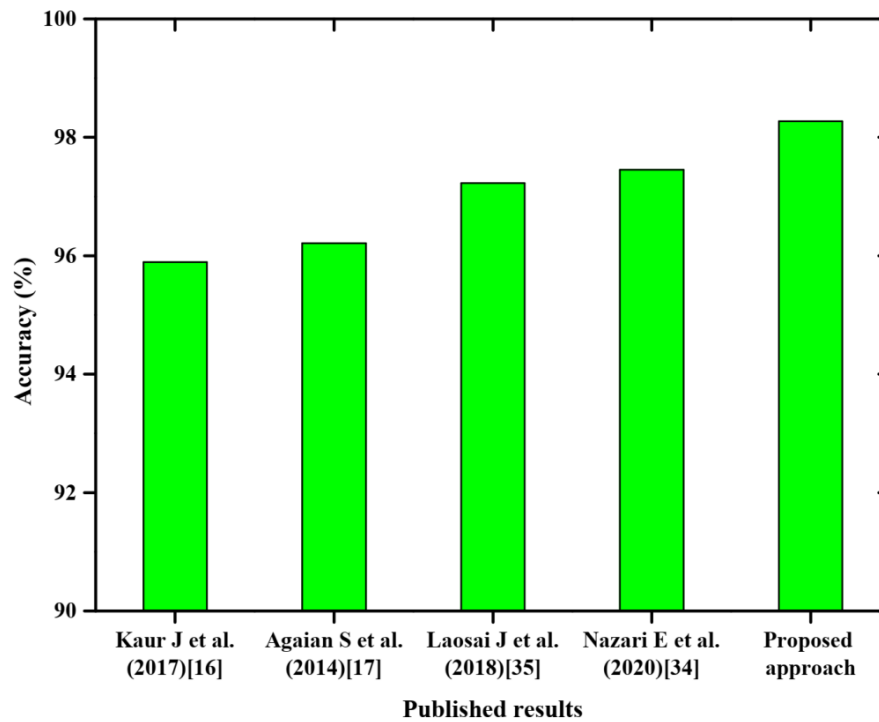


Fig 8: Accuracy for the proposed approach compared with published earlier methods.

Fig 8 demonstrates that the accuracy of the acute myeloid detection. The performance of the accuracy for the proposed approach is compared with the published results such as Kaur J et al. (2017) [16] achieved the accuracy of 95.89%, Agaian S et al. (2014) [17] achieved the accuracy of 96.21%, Laosai J et al. (2018) [35] achieved the accuracy of 97.23%, and Nazari E et al. (2020) [34] achieved the accuracy of 97.45%. When compared with other results, the proposed approach provides better accuracy of 98.27%.

5. CONCLUSION

This paper proposes the AML identification and segmentation method more efficiently for the analysis of the blood cell images. Primarily, the blood cell images are pre-processed to eradicate the unwanted noise from the input image and then provided to the segmentation stage for segmenting the nucleus as well as the masked image. The process of segmentation is conducted by using the modified DRLSE method. Then the image is given to the process of feature extraction and then to the classification process. Here, DCNN with AOA is used for the classification of AML images and normal images. The arithmetic optimization algorithm used in DCNN is to improve the classification accuracy and also enhances the system performance. The performance of this approach is evaluated by using the Munich AML morphology database and CPTAC-AML that consists of 120 images. The performance measures like sensitivity, specificity, accuracy, and precision are utilized for the estimation of the proposed classifier and compared to other methods. In the future, several subtypes of AML have to be classified. Furthermore, the cytoplasm is segmented and the feature is to be extracted for making the system more precise.

REFERENCES

- [1] Jongen-Lavrencic M, Grob T, Hanekamp D, Kavelaars FG, Al Hinai A, Zeilemaker A, Erpelinck-Verschueren CA, Gradowska PL, Meijer R, Cloos J, Biemond BJ. Molecular minimal residual disease in acute myeloid leukemia. *New England Journal of Medicine*. 2018 Mar 29;378(13):1189-99.
- [2] Dillon LW, Hayati S, Roloff GW, Tunc I, Pirooznia M, Mitrofanova A, Hourigan CS. Targeted RNA-sequencing for the quantification of measurable residual disease in acute myeloid leukemia. *Haematologica*. 2019 Feb;104(2):297.
- [3] Rautenberg C, Germing U, Haas R, Kobbe G, Schroeder T. Relapse of acute myeloid leukemia after allogeneic stem cell transplantation: prevention, detection, and treatment. *International journal of molecular sciences*. 2019 Jan;20(1):228.
- [4] Kumar S, Mishra S, Asthana P. Automated detection of acute leukemia using k-mean clustering algorithm. In *Advances in Computer and Computational Sciences 2018* (pp. 655-670). Springer, Singapore.
- [5] Ko BS, Wang YF, Li JL, Li CC, Weng PF, Hsu SC, Hou HA, Huang HH, Yao M, Lin CT, Liu JH. Clinically validated machine learning algorithm for detecting residual diseases with multicolor flow cytometry analysis in acute myeloid leukemia and myelodysplastic syndrome. *EBioMedicine*. 2018 Nov 1;37:91-100.
- [6] Selim AG, Moore AS. Molecular minimal residual disease monitoring in acute myeloid leukemia: challenges and future directions. *The Journal of Molecular Diagnostics*. 2018 Jul 1;20(4):389-97.
- [7] Buccisano F, Maurillo L, Del Principe MI, Di Veroli A, De Bellis E, Biagi A, Zizzari A, Rossi V, Rapisarda V, Amadori S, Voso MT. Minimal residual disease as a biomarker for outcome prediction and therapy optimization in acute myeloid leukemia. *Expert review of hematology*. 2018 Apr 3;11(4):307-13.
- [8] Alagu S, Bagan KB. Computer Assisted Classification Framework for Detection of Acute Myeloid Leukemia in Peripheral Blood Smear Images. In *Innovations in Computational Intelligence and Computer Vision 2021* (pp. 403-410). Springer, Singapore.
- [9] Godwin CD, Zhou Y, Othus M, Asmuth MM, Shaw CM, Gardner KM, Wood BL, Walter RB, Estey EH. Acute myeloid leukemia measurable residual disease detection by flow cytometry in peripheral blood vs bone marrow. *Blood, The Journal of the American Society of Hematology*. 2021 Jan 28;137(4):569-72.
- [10] Craig JW, Hassserjian RP, Kim AS, Aster JC, Pinkus GS, Hornick JL, Steensma DP, Lindsley RC, DeAngelo DJ, Morgan EA. Detection of the KIT D816V mutation in myelodysplastic and/or myeloproliferative neoplasms and acute myeloid leukemia with myelodysplasia-related changes predicts concurrent systemic mastocytosis. *Modern Pathology*. 2020 Jun;33(6):1135-45.
- [11] Su J, Liu S, Song J. A segmentation method based on HMRF for the aided diagnosis of acute myeloid leukemia. *Computer methods and programs in biomedicine*. 2017 Dec 1;152:115-23.
- [12] Aypar U, Smoley SA, Pitel BA, Pearce KE, Zenka RM, Vasmatazis G, Johnson SH, Smadbeck JB, Peterson JF, Geiersbach KB, Van Dyke DL. Mate pair sequencing improves detection of genomic abnormalities in acute myeloid leukemia. *European journal of haematology*. 2019 Jan;102(1):87-96.
- [13] Harjoko A, Ratnaningsih T, Suryani E, Palgunadi S, Prakisyana NP. Classification of acute myeloid leukemia subtypes M1, M2 and M3 using active contour without edge segmentation and momentum backpropagation artificial neural network. In *MATEC Web of Conferences 2018* (Vol. 154, p. 01041). EDP Sciences.

- [14] Matek C, Schwarz S, Spiekermann K, Marr C. Human-level recognition of blast cells in acute myeloid leukaemia with convolutional neural networks. *Nature Machine Intelligence*. 2019 Nov;1(11):538-44.
- [15] Rawat J, Singh A, Bhadauria HS, Virmani J, Devgun JS. Computer assisted classification framework for prediction of acute lymphoblastic and acute myeloblastic leukemia. *Biocybernetics and Biomedical Engineering*. 2017 Jan 1;37(4):637-54.
- [16] Kaur J, Vats I, Verma A. Acute Myeloid Leukemia Detection in WBC Cell Based on ICA Feature Extraction. In *International Conference on Next Generation Computing Technologies 2017 Oct 30* (pp. 722-732). Springer, Singapore.
- [17] Agaian S, Madhukar M, Chronopoulos AT. Automated screening system for acute myelogenous leukemia detection in blood microscopic images. *IEEE Systems journal*. 2014 Mar 13;8(3):995-1004.
- [18] Kumar P, Udwadia SM. Automatic detection of Acute Myeloid Leukemia from microscopic blood smear image. In *2017 International Conference on Advances in Computing, Communications and Informatics (ICACCI) 2017 Sep 13* (pp. 1803-1807). IEEE.
- [19] Jayaraman T, Reddy S, Mahadevappa M, Sadhu A, Dutta PK. Modified distance regularized level set evolution for brain ventricles segmentation. *Visual Computing for Industry, Biomedicine, and Art*. 2020 Dec;3(1):1-2.
- [20] Li CM, Xu CY, Gui CF, Fox MD (2005) Level set evolution without re-initialization: a new variational formulation. In: *Abstracts of 2005 IEEE computer society conference on computer vision and pattern recognition*. IEEE, San Diego
- [21] Phillips CL (1999) The level-set method. *MIT Undergrad J Math* 1:155–164
- [22] Lu Z, Carneiro G, Bradley AP (2015) An improved joint optimization of multiple level set functions for the segmentation of overlapping cervical cells. *IEEE Trans Image Process* 24(4):1261–1272.
- [23] Dongye CL, Zheng YG, Jiang DH (2014) A fast global minimization of region-scalable fitting model for medical image segmentation. *J Softw* 9(2): 280–286.
- [24] Bai PR, Song DD, Bi LJ, Li L, Qi T (2015) A novel integration scheme based on mean shift and region-scalable fitting level set for medical image segmentation, *Abstracts of the 2015 3rd international conference on machinery, materials and information technology applications*. Atlantis press, Qingdao.
- [25] Jha KK, Dutta HS. Mutual information-based hybrid model and deep learning for acute lymphocytic leukemia detection in single cell blood smear images. *Computer methods and programs in biomedicine*. 2019 Oct 1;179:104987.
- [26] Abualigah L, Diabat A, Mirjalili S, Abd Elaziz M, Gandomi AH. The arithmetic optimization algorithm. *Computer methods in applied mechanics and engineering*. 2021 Apr 1;376:113609.
- [27] M.K. Habib, A.K. Cherri, Parallel quaternary signed-digit arithmetic operations: addition, subtraction, multiplication and division, *Opt. Laser Technol.* 30 (8) (1998) 515–525.
- [28] <https://wiki.cancerimagingarchive.net/pages/viewpage.action?pageId=61080958#bcab02c187174a288dbcbf95d26179e8>
- [29] <https://wiki.cancerimagingarchive.net/display/Public/CPTAC-AML>
- [30] Wiharto W, Suryani E, Putra YR. Classification of blast cell type on acute myeloid leukemia based on image morphology of white blood cells.
- [31] Setiawan A, Harjoko A, Ratnaningsih T, Suryani E, Palgunadi S. Classification of cell types in Acute Myeloid Leukemia (AML) of M4, M5 and M7 subtypes with support vector machine classifier.

In 2018 international conference on information and communications technology (ICOIACT) 2018 Mar 6 (pp. 45-49). IEEE.

- [32] Harjoko A, Ratnaningsih T, Suryani E, Palgunadi S, Prakisyah NP. Classification of acute myeloid leukemia subtypes M1, M2 and M3 using active contour without edge segmentation and momentum backpropagation artificial neural network. In MATEC Web of Conferences 2018 (Vol. 154, p. 01041). EDP Sciences.
- [33] Ramya, V.J. and Lakshmi, S., 2022. Acute myelogenous leukemia detection using optimal neural network based on fractional black-widow model. *Signal, Image and Video Processing*, 16(1), pp.229-238.
- [34] Nazari E, Farzin AH, Aghemiri M, Avan A, Tara M, Tabesh H. Deep Learning for Acute Myeloid Leukemia Diagnosis. *Journal of Medicine and Life*. 2020 Jul;13(3):382.
- [35] Laosai J, Chamnongthai K. Classification of acute leukemia using medical-knowledge-based morphology and CD marker. *Biomedical Signal Processing and Control*. 2018 Jul 1;44:127-37.
- [36] Jayaraman T, Reddy S, Mahadevappa M, Sadhu A, Dutta PK. Modified distance regularized level set evolution for brain ventricles segmentation. *Visual Computing for Industry, Biomedicine, and Art*. 2020 Dec;3(1):1-2.